Mitral valve patient-specific finite element modeling from 3-D real time echocardiography: a potential new tool for surgical planning

E. Votta[1], A. Arnoldi[2], A. Invernizzi[2], R. Ponzini[2], F. Veronesi[3], G. Tamborini[4], M. Pepi[4], F. Alamanni[4], A. Redaelli[1], E.G. Caiani[1]

[1]Bioengineering Department, Politecnico di Milano, Milano, Italy
emiliano.votta@polimi.it
alberto.redaelli@polimi.it
Enrico.caiani@polimi.it
[2]C.I.L.E.A., Segrate (MI), Italy
arnoldialice@hotmail.com
invernizzi@cilea.it
ponzini@cilea.it
[3]University of Bologna, Bologna, Italy
federico.veronesi@unibo.it
[4]Centro Cardiologico Monzino IRCCS, Milano, Italy
gloria.tamborini@ccfm.it
mauro.pepi@ccfm.it
francesco.alamanni@ccfm.it

Mitral valve (MV) physiopathological function and the effects of surgical repair can be studied through finite element models (FEMs). However, this approach assumes idealized morphology and boundary conditions limiting the analysis to paradigmatic scenarios and precluding patient-specific surgical planning. To overcome this limitation, we integrated into a MV FEM the patient-specific information about leaflets, annulus and papillary muscles geometry and dynamics, obtained from real-time 3D echocardiography. An ad-hoc web platform was created to facilitate FEM development from remote users, and grant access to parallel computing facilities. This approach was tested simulating MV closure in three normal subjects. Modelled valvular dynamics and quantitative results were consistent with experimental findings from literature. FEMs implementation required about 6 min, while simulations required about 7.5 hours on 32 parallel CPUs. Our approach appears reliable, reproducible and reasonably fast and may constitute the basis for the development of patient-specific tools for MV surgery.

Introduction

The high prevalence of mitral valve (MV) pathologies that require surgical repair has led to increasingly more sophisticated techniques and implantable devices, whose conceiving and application need careful design and testing. This process can benefit from the use of finite element models (FEMs), which allow analyzing MV

biomechanics as a result of multiple co-existing factors, possibly isolating the effect of each of them and, ones validated, can be used as a predictive tool. FEMs have already been applied to study MV normal function [1-3], the biomechanics underlying MV diseases [1] and effects of surgical corrections [4-7]. However, to obtain a patient-specific model that could be used for surgical planning, MV morphology, tissues mechanical response, dynamic boundary conditions and interaction between the MV and surrounding blood have to be realistically represented. In particular, current MV FEMs, based on animal or ex vivo data, assume an idealized, symmetrical valvular structure and neglect the dynamic contraction of the mitral annulus (MA) and the papillary muscles (PMs).

Real time 3-D echocardiography (RT3DE) offers the potential to non-invasively assess MV structures over time, thus providing the information needed to overcome the abovementioned limitations [8]. Our aim was to explore the feasibility to integrate into a MV structural FEM the patient-specific information about leaflets, annulus and papillary muscles geometry and dynamics, obtained by analysis of RT3DE. In addition, an ad-hoc web platform was created to facilitate FEM development from potential remote users by an easy-to-use graphical user interface (GUI), and grant access to extended computational resources. In order to test the repeatability and robustness of our approach, we applied it to the analysis of the MV biomechanics in three normal subjects.

Finite Element Model Implementation From RT3DE

Real-Time 3D echocardiography

Transthoracic RT3DE imaging was performed (iE33, Philips, Andover, MA) from the apical window using a fully sampled matrix-array transducer (X3), with the subject in the left lateral decubitus position. RT3DE datasets were acquired using the wide-angled mode at high frame rate (31 Hz), wherein 8 wedge-shaped subvolumes were obtained during 8 cardiac cycles during a single breath hold with ECG gating. Three normal subjects were analyzed (2 males, 29 and 40 years old; 1 female, 49 years old).

RT3DE datasets were analyzed using custom software [9]. In the end-diastolic (ED) frame, PMs tips were manually identified by rotating the cut plane around the MA center, until the tip of each PM was best visualized and its position defined. On the MA, two points, one on each side of the MA, were manually initialized in 12 evenly-rotated (15° step) long-axis cut planes on the ED frame. Then, the initialized points were automatically tracked frame-by-frame in 3D space, using optical flow and region-based matching techniques. The tracked points were displayed in each frame to verify their position, and manual corrections were performed when necessary. Leaflets tilting angle and annulus-to-free edge width were measured in an apical 4-chamber cut plane.

Mitral Valve Geometrical Model

The MV ED configuration was chosen as the unstressed one. The geometrical model (Figure 1.a) was implemented defining i) the annular profile, by interpolation of the 36 points selected on the MA in the ED frame using RT3DE (Figure 1.b); ii) PMs tips, defined as circular structures with 3 mm diameter, centred in the two points selected in the ED frame (Figure 1.c); iii) the leaflets, whose profile, based on ex-vivo data from the literature [10], was adapted to the measured annulus-to-free edge size and spatial orientation (Figure 1.d); iv) 39 branched chordae tendineae of three orders. The number of chordae, the corresponding branched structure and insertion sites on the leaflets were defined in accordance to ex vivo findings [11]. A constant thickness of 1.32 mm and 1.26 mm was defined for anterior and posterior leaflet, respectively. Two transitional commissural zones with a thickness of 1.29 mm were also identified. Constant cross-section area values of 0.4, 1.15 and 0.79 mm^2 were assigned to 1st order, strut and basal chordae, respectively.

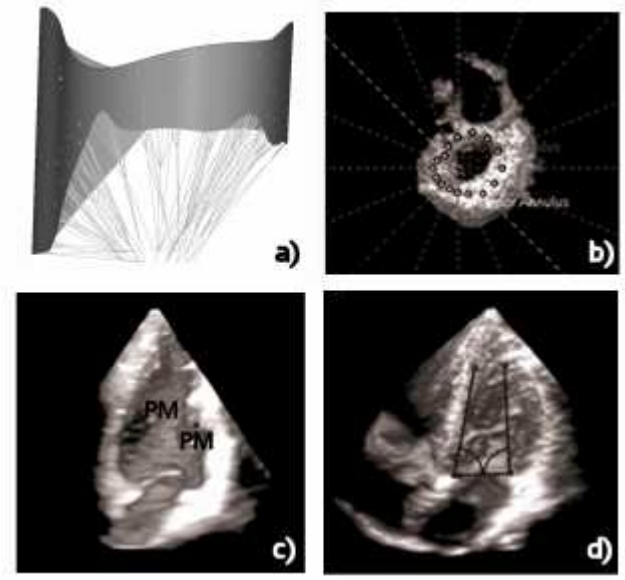

Fig. 1. a) Valve geometrical model, b) ED annular profile, c) papillary muscles and d) leaflets inclination were detected on the ED ultrasound frame.

Modelling of Tissues Mechanical Properties and Dynamic Boundary Conditions

All tissues were assumed non-linear and elastic. Their mechanical response was described by means of proper strain energy potentials. Leaflets anisotropic response was accounted for by means of a Fung-like strain energy potential [8]. Chordae tendineae response was assumed isotropic. A second order polynomial strain energy potential was used for 1st order chordae; a fifth order Ogden strain energy function

was used for 2nd and 3rd order chordae. The constitutive parameters were defined via mean-square interpolation of data from the literature [12, 13].

The dynamic contraction of MA and PMs was modelled via kinematic boundary conditions, i.e. imposed as nodal displacements. For each RT3DE frame, the position of the nodes defining the MA profile was derived and used as a model constraint. The motion of PMs tips was estimated from RT3DE data and through a geometrical model based on in vivo data from animal models [14]. To simulate the effect of blood pressure from ED to systolic peak (SP), a physiological time-dependent transvalvular pressure drop, up to 120 mmHg, was applied on the leaflets.

Integration of FEMs Set-up and Simulations into an ad-Hoc Virtual Platform

In order to make the set-up of MV FEMs semi-automated and accessible to users with a pure clinical background, we developed, in collaboration with CILEA (Consorzio Interuniversitario Lombardo per l'Elaborazione Automatica), the Mitral Valve Models Reconstructor (MVMR) software tool. This software is an ad-hoc Python-based graphic user interface (GUI), built upon a high performance graphic server (ThinAnyWhere software (Mercury International Technology) that allows a remote non-expert user to easily: i) upload pre-processed RT3DE data, consisting in ASCII files containing the spatial time-dependent coordinates of the MV previously tracked points; ii) reconstruct and discretize the MV 3D geometrical model. At this level the user can visualize and eventually re-tune the reconstructed geometry model (figure 2).

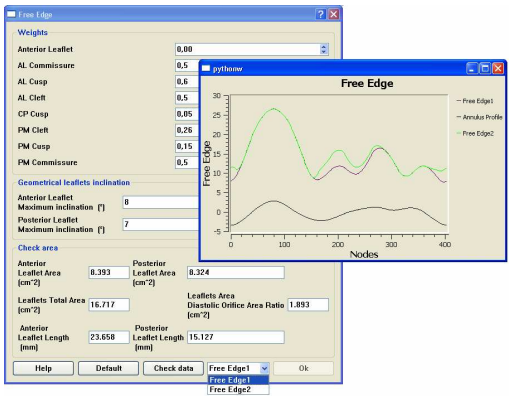

Fig. 2. Example of the functionalities: widget for leaflets definition. The user can identify several configurations for leaflets free edge, check them and choose the more realistic one.

After the geometry model preparation the user can, by means of the software tool, can: iii) define an input file describing the complete MV FEM for ABAQUS/Explicit 6.7-1 (Dessault Systèmes SIMULIA Corp.); iv) submit to a high performance computing (HPC) environment the overall numerical simulations. The HPC server (namely lagrange.cilea.it) is composed of 208 2-ways nodes, Intel Xeon QuadCore at 3.16 GHz equipped with 16 GB RAM/node. The numerical simulations use the ABAQUS/Explicit 6.7-1 solver and then by means of an e-mail notification service

(developed upon PBS-Professional queuing system (Altair Engineering.Inc) the user can be informed of the status of numerical simulations. Finally the FEMs results can be post-processed via ABAQUS/Viewer launched by the MVMR software tool.

Results and discussion

MV Biomechanical Analysis

The patient-specific MVs obtained from the three analyzed normal subjects showed similar features in their biomechanical response. Closure dynamics and leaflets coaptation were consistent with in-vitro observations: complete coaptation was obtained for an 18 mmHg transmitral pressure [15] and, accordingly with clinical observations, the coaptation region corresponded to the leaflets rough zone.

The MV tensile state was analysed focusing on SP, when the pressure load is maximal. Leaflets strains (figure 3) reflected tissue anisotropic response, much stiffer in the direction parallel to the MA than orthogonal to it. In particular, in the belly of the anterior leaflet, stretch ratios in the two directions averaged on the three subjects ranged from 1.11 to 1.15 and from 1.29 to 1.41, respectively, in good agreement with experimental data [16].

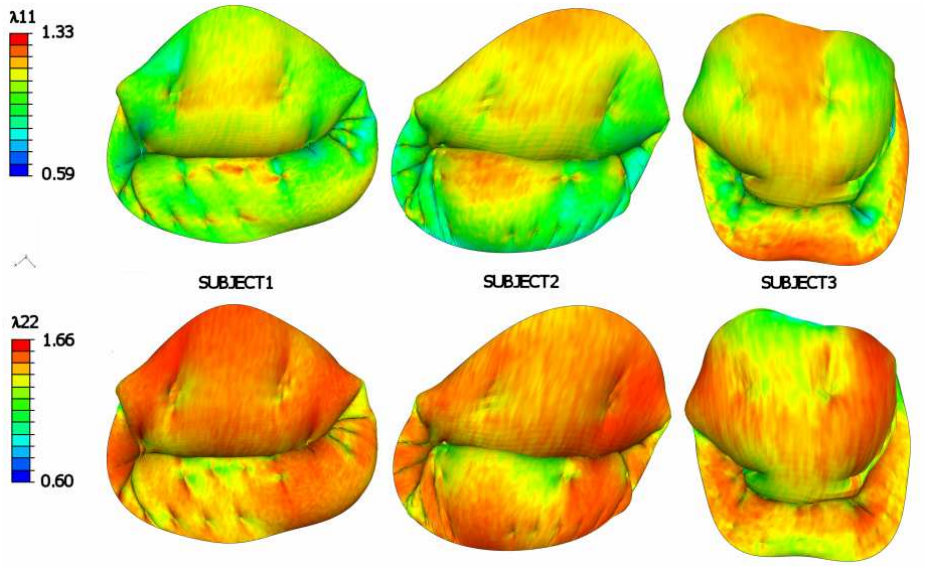

Fig. 3. Stretch ratios computed in the direction parallel to the annulus (λ11) and perpendicular to it (λ22) for the three subjects. Valves are depicted in an atrial view.

Leaflets maximum principal stresses were computed (Figure 4). Their distribution reflected the asymmetry of the initial geometrical model. The anterior leaflet resulted more stressed than the posterior one; peak values of 550 kPa were computed next to

the fibrous trigones on the MA, or at the insertion of strut chordae, depending on the particular subject. The occurrence of stress peak values at these locations appears consistent with MV functional anatomy: fibrous trigones are known as very robust structures where the surrounding soft tissues are anchored.

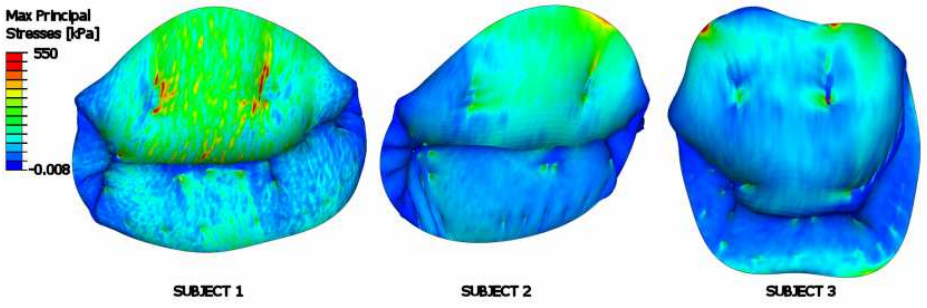

Fig. 4. Leaflets maximum principal stresses at the systolic peak (atrial view).

As regards tensions in the subvalvular apparatus, PMs forces evolved during closure following the transvalvular pressure. Peak values ranged from 4 to 6.5 N. As depicted in figure 5, such tensions were unevenly transmitted to chordae tendineae throughout the simulated timeframe: the average load on a single chorda was highest in the strut chordae (up to 1.02 N at the SP) and much lower in first order chordae (0.17 N at the SP), although these, being many more, altogether bore the major load fraction, consistently with experimental observations from the literature [10].

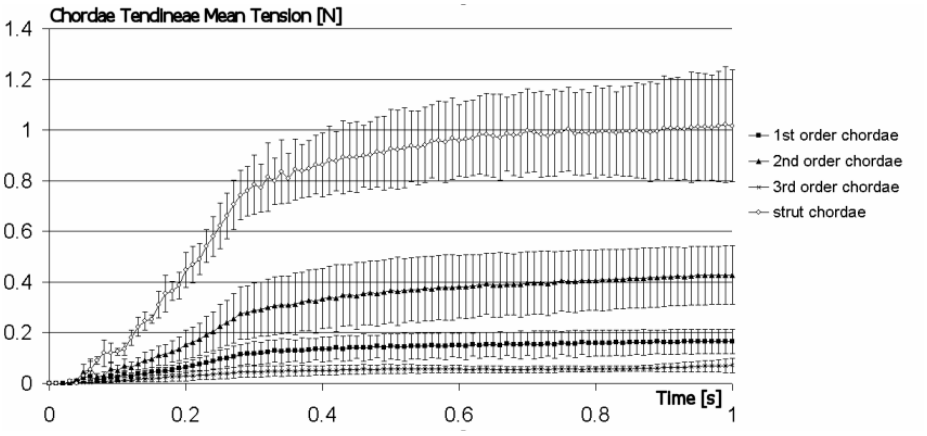

Fig. 5. Time course of chordae tendineae tensions averaged on chordae of the same type. Symbols represent the mean value for the three analyzed subjects. Error bars represent standard deviations on the three subjects.

Table 1 summarizes the distribution of chordae tendineae tensions at the SP and compares them with experimental values reported in [17]. Computational and

experimental values are comparable for all types of chordae, with the only exception of 3rd order chordae. However, these are subject to great inter-subject variability and originate from very different locations on the ventricular inner wall. The strategy herein adopted to model them may have biased the results.

MVMR Performance

The MVMR virtual platform allowed the semi-automated implementation of MV FEMs in about 6 minutes, against the about 2 hours needed for the manual implementation. Moreover, the access to a HPC environment allowed a huge decrease in computational costs for numerical simulations: on 16 and 32 parallel CPUs these lasted 13 and 7.5 hours, respectively, against the 81 hours needed on a single CPU.

Table 1. Computed systolic peak chordae tensions, compared to in vitro data from literature [16]. In [16] further distinctions are made within 1st order chordae, depending on their site of insertion on the leaflets, which is here reported in brackets.

Chordae Type		Systolic Peak Tension [N]	
		FEM Data	In Vitro Data [16]
1° Order Chordae	SUBJECT1	0.495 ± 0.394	0.18 ± 0.16 (anterior)
	SUBJECT2	0.447 ± 0.304	0.08 ± 0.11 (posterior)
	SUBJECT3	0.221 ± 0.175	0.40 ± 0.31 (commissural)
2nd Order Chordae	SUBJECT1	0.607 ± 0.292	0.29 ± 0.14 (posterior)
	SUBJECT2	0.644 ± 0.461	
	SUBJECT3	0.374 ± 0.163	
3rd Order Chordae	SUBJECT1	0.127 ± 0.176	0.48 ± 0.25
	SUBJECT2	0.057 ± 0.035	
	SUBJECT3	0.086 ± 0.058	
Strut Chordae	SUBJECT1	1.090 ± 0.253	1.11 ± 0.57
	SUBJECT2	0.855 ± 0.047	
	SUBJECT3	0.708 ± 0.258	

Limitations and Future Developments

Despite the promising results it provided, our modeling strategy still suffers from some limitations: although in our opinion these are not likely to controvert the validity of computational results, they will require further efforts to be overcome.

First, the reconstruction of a truly patient-specific MV model, the main issue is in the definition of the sub-valvular apparatus and is due to limitations inherent in RT3DE. On the one hand, it is rare to obtain datasets that allow tracking both PMs throughout the entire simulated timeframe, since these often fall out of the acquired volume due to their motion. On the other hand, from RT3DE it is currently not possible to exactly reconstruct the chordal apparatus and to identify chordae branches

and insertions. For these reasons PMs motion and chordae tendineae morphology were modeled on the basis of data from the literature and through geometrical criteria. Future efforts will be focused on further testing such criteria and assessing the sensitivity of computational outcomes to changes in chordae morphology and PMs motion within a physiological range.

Second, the model developed by our strategy is purely structural: the action of blood on the leaflets is modeled by applying a time-dependent pressure on them and not by modeling the actual fluid-structure interaction. Thus, the presence and the effects of local vortexes in the blood, which are known to influence leaflets dynamics and could induce local decreases in pressure and leaflets stresses, are not accounted for. Including this feature in the model would be a challenging and interesting development of our work.

Third, independently of the abovementioned considerations, further testing of our modeling strategy on a wider group is mandatory, since three subjects may be not be fully representative of the standard physiological population. We are currently performing acquisitions on new healthy subjects to increase the group size and we are planning to apply our methods on the new datasets in the next future.

Conclusions

With this study, a novel approach to obtain a MV FEM with beyond-state-of-the-art features was defined and tested. Results suggest that the use of RT3DE allows overcoming previous MV FEMs limitations related to the description of MV morphology and MA and PMs motion, thus allowing for patient-specific customization of the FEM, which is one of the mandatory conditions to use FEMs in surgical planning. Moreover, the MVMR provided an easy-to-use interface for FEMs handling and made the time needed for models set-up and simulations short enough to be compatible with the timing of surgical therapies. Both these criteria were fulfilled thanks to the virtual platform we implemented. Although further testing on more subject-specific data is mandatory, this strategy may be at the basis for the development of a patient-specific modeling tool to be applied in the clinical settings or for surgical planning.

Acknowledgements

The research leading to these results has received funding from the European Community's Seventh Framework Programme (FP7/2007-2013) under grant agreement n° FP7-224635 and from the Italian Ministry of Education, University and Research (PRIN 2007 funds, SurgAid Project).

References

1. Kunzelman, K.S., Einstein, D.R., Cochran, R.P.: Fluid-structure interaction models of the mitral valve: function in normal and pathological states. Philos. Trans. R. Soc. Lond. B Biol. Sci. 362, 1393--1406 (2007)
2. Lim, K.H., Yeo, J.H., Duran, C.M.: Three-dimensional asymmetrical modeling of the mitral valve: a finite element study with dynamic boundaries. J. Heart Valve Dis. 14, 386--392 (2005)
3. Prot, V., Haaverstad, R., Skallerud, B.: Finite element analysis of the mitral apparatus: annulus shape effect and chordal force distribution. Biomech. Model. Mechanobiol. 8, 43--55 (2009)
4. Cochran, R.P., Kunzelman, K.S.: Effect of papillary muscle position on mitral valve function: relationship to homografts. Ann. Thorac. Surg. 66, S155--S161 (1998)
5. Votta, E., Maisano, F., Soncini, M., Redaelli, A., Montevecchi, F.M., Alfieri, O.: 3-D computational analysis of the stress distribution on the leaflets after edge-to-edge repair of mitral regurgitation. J. Heart Valve Dis. 11, 810--822 (2002)
6. Dal Pan, F., Donzella, G., Fucci, C., Schreiber, M.: Structural effects of an innovative surgical technique to repair heart valve defects. J. Biomech. 38, 2460--2471 (2005)
7. Votta, E., Maisano, F., Bolling, S.F., Alfieri, O., Montevecchi, F.M., Redaelli, A. The Geoform disease-specific annuloplasty system: a finite element study. Ann. Thorac. Surg. 84, 92--101 (2007)
8. Votta, E., Caiani, E., Veronesi, F., Soncini, M., Montevecchi, F.M., Redaelli, A.: Mitral valve finite-element modelling from ultrasound data: a pilot study for a new approach to understand mitral function and clinical scenarios. Philos. Transact. A Math. Phys. Eng. Sci. 366, 3411--34 (2008)
9. Veronesi, F., Corsi, C., Sugeng, L., Caiani, E.G., Weinert, L., Mor-Avi, V., Cerutti, S., Lamberti, C., Lang, R.M.: Quantification of mitral apparatus dynamics in functional and ischemic mitral regurgitation using real-time 3-dimensional echocardiography. J. Am. Soc. Echocardiogr. 21, 347--54 (2008)
10. Kunzelman, K.S., Cochran, R.P., Verrier, E.D., Eberhart, R.C.: Anatomic basis for mitral valve modelling. J. Heart Valve Dis. 3, 491--496 (1994)
11. Lam, J.H.C., Ranganathan, N., Silver, M.D.: Morphology of the human mitral valve. I. Chordae tendinae: a new classification. Circulation 41, 449--458 (1970)
12. Kunzelman, K.S., Cochran, R.P.: Mechanical properties of basal and marginal mitral valve chordae tendineae. ASAIO Trans. 36, M405--M408 (1990)
13. Liao, J., Vesely, I.: A structural basis for the size-related mechanical properties of mitral valve chordae tendineae. J. Biomech. 36, 1125-1133 (2003)
14. Dagum, P., Timek, T.A., Green, G.R., Lai, D., Daughters, G.T., Liang, D.H., Hayase, M., Ingels, N.B., Miller, D.C.: Coordinate-Free analysis of mitral valve dynamics in normal and ischemic hearts. Circulation 102, III62--69 (2000)
15. Timek, T., Glasson, J.R., Dagum, P., Green, G.R., Nistal, J.F., Komeda, M., Daughters, G.T., Bolger, A.F., Foppiano, L.E., Ingels, N.B. Jr, Miller, D.C.: Ring annuloplasty prevents delayed leaflet coaptation and mitral regurgitation during acute left ventricular ischemia. J. Thorac. Cardiovasc. Surg. 119, 774--783 (2000)
16. Sacks, M.S., He, Z., Baijens, L., Wanant, S., Shah, P., Sugimoto, H., Yoganathan, A.P.: Surface strains in the anterior leaflet of the functioning mitral valve. Ann. Biomed. Eng. 30, 1281--1290 (2002)
17. Jimenez, J.H., Soerensen, D.D., He, Z., Ritchie, J., Yoganathan, A.P.: Mitral valve function and chordal force distribution using a flexible annulus model: an in vitro study. Ann. Biomed. Eng. 33, 557--566 (2005)